Taylor & Francis
Taylor & Francis Group

Ships and Offshore Structures

ISSN: (Print) (Online) Journal homepage: https://www.tandfonline.com/loi/tsos20

FELA evaluation of undrained bearing capacity of cutting edge of circular open caisson

Jitesh T. Chavda, Wittaya Jitchaijaroen, Suraparb Keawsawasvong & Phadungsak Rattanadecho

To cite this article: Jitesh T. Chavda, Wittaya Jitchaijaroen, Suraparb Keawsawasvong & Phadungsak Rattanadecho (2023): FELA evaluation of undrained bearing capacity of cutting edge of circular open caisson, Ships and Offshore Structures, DOI: 10.1080/17445302.2023.2225952

To link to this article: https://doi.org/10.1080/17445302.2023.2225952

Published online: 21 Jun 2023.

SHIPS AND OFFSHORE STRUCTURES
https://doi.org/10.1080/17445302.2023.2225952

Taylor & Francis
Taylor & Francis Group

RAPID COMMUNICATION

FELA evaluation of undrained bearing capacity of cutting edge of circular open caisson

Jitesh T. Chavda [a], Wittaya Jitchaijaroen [b], Suraparb Keawsawasvong [c] and Phadungsak Rattanadecho [d]

[a]Department of Civil Engineering, Sardar Vallabhbhai National Institute of Technology, Surat, India; [b]Department of Civil Engineering, Faculty of Engineering, Thammasat School of Engineering, Thammasat University, Pathumthani, Thailand; [c]Research Unit in Sciences and Innovative Technologies for Civil Engineering Infrastructures, Department of Civil Engineering, Faculty of Engineering, Thammasat School of Engineering, Thammasat University, Pathumthani, Thailand; [d]Center of Excellence in Electromagnetic Energy Utilization in Engineering (C.E.E.E.) Department of Mechanical Engineering, Faculty of Engineering, Thammasat School of Engineering, Thammasat University, Pathumthani, Thailand

ABSTRACT

Circular open caissons are deep foundations sunk into the ground utilising the self-weight of cutting edge and steining as driving force along with the subsequent failure of soil in bearing. During the sinking of the caisson, the clay in contact with the cutting edge is subjected to undrained loading and the controlled sinking of the caisson can be achieved by evaluating the undrained bearing capacity of the cutting edge. In the study, the undrained bearing capacity factor (*N*) of the cutting edge for varying cutting angle (*b*), radius ratio of the caisson (r_i/r_o), full embedment of the caisson (*d*), removal of soil within the caisson (*d'*), and different roughness (*α*) conditions of the steining are evaluated using finite element limit analysis (FELA). The factors affecting the undrained stability of caisson considering all practical scenarios are addressed and presented as charts to be used in practice.

ARTICLE HISTORY
Received 25 February 2023
Accepted 11 June 2023

KEYWORDS
Undrained bearing capacity factor; cutting edge; open caisson; FELA; offshore foundation; undrained cohesion

Notations

B	width of the cutting edge of open caisson
c	cohesion of soil
d	embedment of caisson
d'	removal of soil within caisson
E	modulus of elasticity
FELA	finite element limit analysis
LB	lower bound
N_c, N_q and N_γ	bearing capacity factors of the strip footing
N_c*, N_q* and N_γ*	modified bearing capacity factors of the open caisson
N	undrained bearing capacity factor
q	surcharge above the cutting-edge level
q_u	ultimate bearing capacity of the cutting edge of open caisson
r_i	inner radius
r_o	outer radius
r_i/r_o	radii ratio
SOCP	second-order cone programming
UB	upper bound
α	base roughness between footing and soil
β	cutting angle
ϕ	friction angle of soil
γ	unit weight of soil
ν	Poisson's ratio

1. Introduction

Open caissons are deep foundations adopted as a choice of foundation for offshore, onshore and inland structures (Chakrabarti et al. 2006; Esteban Lefler and Rey Romero 2009; Matsuda et al. 2016; Dong et al. 2023; Jiang et al. 2023). They are sunken to the required depth using the self-weight of the cutting edge and subsequent raising of steining (Nonveiller 1987). The open caisson has different shapes in plan like rectangle, square, circular, dumb-bell and in-plan grids of steining (Nayak 1985). Usually, the circular shape is adopted and is defined by the radius ratio which is the ratio of the inner radius to the outer radius of the cutting edge (Chavda and Dodagoudar 2018). Practically the radius ratio (r_i/r_o) of caisson can vary from 0.25 to 0.8, where r_i is inner radius and r_o is outer radius of cutting edge of caisson. The larger radii ratios ($r_i/r_o \sim$ 0.8) are adopted for stormwater tanks, attenuation tanks, launch and reception pits for tunnel boring machines, etc. (e.g. Nonveiller 1987; Allenby et al. 2009; Yao et al. 2014; Royston et al. 2016; Sheil et al. 2018); whereas, the lower radii ratios (r_i/r_o ~0.25–0.5) are usually adopted as foundation for bridge piers or offshore structures. The cutting edge has an inclined face defined by an angle β varying from 30° to 45° (IS: 9527, Part 1 1981; IS: 3955 1965; IRC: 78 2000; Tomlinson 2001; Chavda and Dodagoudar 2022b). The caissons are used in inundated conditions to support bridges over rivers (Dammala et al. 2017). When caissons are sunken in the river bed or sea bed, if the soil is clay, the sinking of caisson is governed by the failure of clay subjected to undrained loading and the roughness conditions of steining. In such cases, estimating the stability of a caisson at every stage of sinking is important to have control over the rate of sinking of the caisson.

The uniform sinking of caisson is usually achieved when the soil in contact with the cutting edge fails in shear together radially. The evaluation of bearing capacity of the cutting edge will help in planning the controlled sinking. The bearing capacity of cutting edge has been investigated using experiments (Chavda et al. 2020; Chavda and Dodagoudar 2022a), slip line method (Berezantsev 1952; Solov'ev 2008; Yan et al. 2011), finite element method (Sheil and Templeman 2022; Chavda and Dodagoudar 2022b) and finite element limit analysis (Templeman et al. 2021; Sheil and Templeman 2022; Royston et al. 2022a). There are several practical possible cases of caisson sinking in clayey soil starting from only cutting edge embedded in soil, cutting edge and steining complete embedded in soil, embedded caisson with soil removed within caisson, with different roughness conditions ($\alpha = 0$ to 1) of steining (Chavda and Dodagoudar 2022a). The bearing capacity of the cutting edge in soil will vary based on the above conditions. Therefore, this study addresses the undrained bearing capacity of cutting edge

CONTACT Suraparb Keawsawasvong ksurapar@engr.tu.ac.th Research Unit in Sciences and Innovative Technologies for Civil Engineering Infrastructures, Department of Civil Engineering, Faculty of Engineering, Thammasat School of Engineering, Thammasat University, Pathumthani 12120, Thailand

of circular open caisson considering all practical scenarios on different conditions of caisson as discussed in the proceeding section.

2. Practical scenarios and proposed study

There are five cases that represent the sequence of the open caisson construction (refer Figure 1). First, **Case A** represents the step that the open caisson is merely tipped into the ground surface, where only the cutting edge is considered i.e. the cutting edge is fully embedded. The interface at the contact between the cutting edge and surrounding soil is fully rough ($\alpha = 1$). Second, **Case B** is carried out to simulate the situation that the open caisson is embedded into soil and the inside soil is not excavated yet. In this case, the embedded depth denoted by d is taken into account. Practically, due to the use of interface lubrication during caisson sinking (Royston et al. 2016, 2022a, 2022b), the interface at the sided wall (above the cutting edge) is assumed to be fully smooth ($\alpha = 0$; smooth steining) whereas that of the cutting edge is still fully rough ($\alpha = 1$). This case considers only the resistance of cutting edge present at greater embedment. Third, **Case C** is the case that the inside soil is partially excavated, where the excavation depth is defined by d'. Note that the setting of the interface in Case C is similar to that in Case B. Fourth, **Case D** shows a case that is similar to Case B, but the interface at the sided wall of this case is assumed to be fully rough ($\alpha = 1$; rough steining) to simulate the case that interface lubrication is not employed in the construction of open caisson. Finally, **Case E** represents the case that is similar to Case C (partially excavated), but the sided wall interface is set to be fully rough ($\alpha = 1$).

The present study focuses on the stability of the circular caisson embedded in clayey soil subjected to undrained loading using finite element limit analysis. The undrained bearing capacity factor N for the cutting edge is evaluated corresponding to the above possible cases. The circular caissons have cutting edge with cutting angles $\beta = 30°$ and 45°, the radius ratio varying from 0.25 to 0.9, the width of the cutting edge same as steining as $B = r_o - r_i = 1$ m, the embedment of caisson varying from $d = 0B$ to $20B$ and the removal of soil within caisson varying from $d' = 0B$ to $20B$. This study will help in understanding the undrained response of caisson in clay and the factors affecting the stability of sinking of caisson in undrained conditions.

3. Finite element limit analysis

The classic bearing capacity factors (i.e. N_c, N_q and N_γ) were proposed by Terzaghi (1943) for the design of the ultimate vertical load of strip foundations. Later, to capture the impact of several shapes of foundations, Caquot and Kérisel (1953), Hansen (1961), Meyerhof (1963), de Beer (1970) and Vesic (1973) presented the modified bearing capacity factors for predicting the bearing capacity of circular, rectangular and other shapes. In the present study, the bearing capacity of the cutting edge of the open caisson is expressed as defined by Equation (1) below.

$$q_u = cN_c^* + qN_q^* + (r_o - r_i)\,\gamma N_\gamma^* \tag{1}$$

where q_u is the ultimate bearing capacity of the cutting edge of the open caisson, c is the cohesion of soil, q is the surcharge above the cutting-edge level, γ is the unit weight of the soil, $B = r_o - r_i$ is the width of the cutting edge of the open caisson, N_c^*, N_q^*, and N_γ^* are the modified bearing capacity factors of the open caisson. The same equation (Equation (1)) is used by Chavda and Dodagoudar (2022b) for the evaluation of the bearing capacity factors for cutting edge of caissons.

This study considers only the undrained condition of the bearing capacity of the cutting edge of the open caisson. As a result, only the N_c^* factor is taken into account and the N_q^* and N_γ^* factors are not considered in the present study. Based on the Griffiths's approach (Griffiths 1982), the N_c^* factor can be acquired by setting the unit weight of soil and surcharge equal to zero (i.e. $\gamma = 0$ and $q = 0$). Thus, the following equation can be obtained for evaluating N_c^* as

$$N_c^* = \frac{q_u}{c} \tag{2}$$

In the present study, the cutting angle β is 30° and 45°. These selected values of β are based on the finding by Chavda et al. (2020) and Chavda and Dodagoudar (2021). They found that, by using the

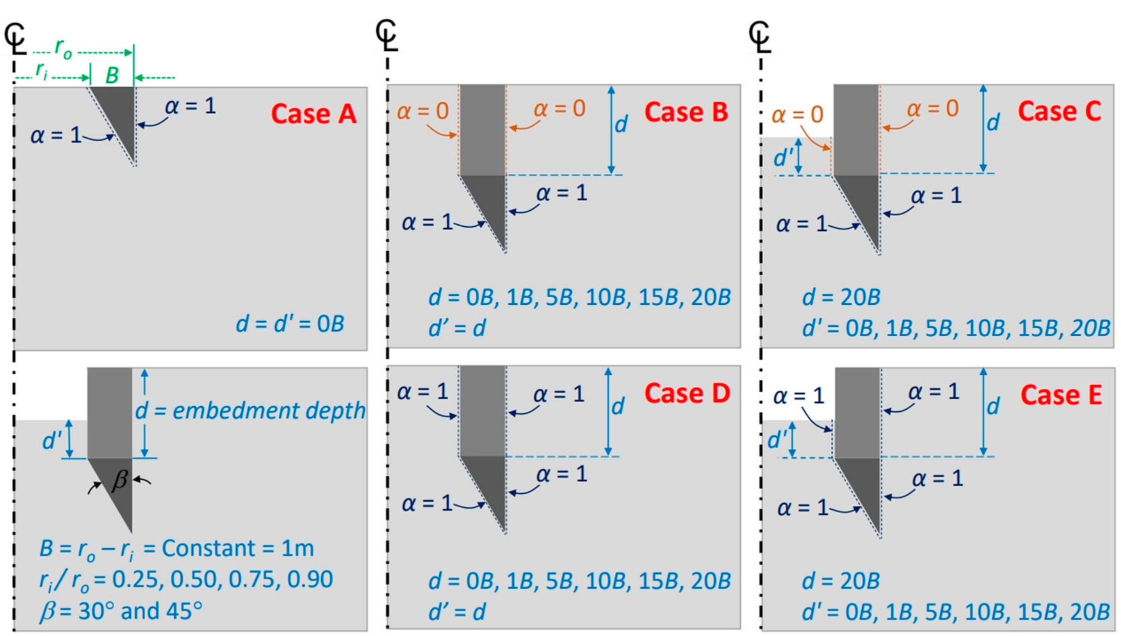

Figure 1. Schematic representation of cases considered in the study for determination of undrained capacity of cutting edge of circular open caisson. (This figure is available in colour online.)

image analysis, the impact of the cutting angle is significant when the β is about 30° to 45°. It should be also noted that the width $B = r_o - r_i$ is set to be constant as 1 m in the analysis. The undrained bearing capacity factor is represented as N in the study. Note that $N = N_c^*$.

The five cases as presented in Figure 1 are investigated using the finite element limit analysis (FELA) which is the most useful numerical technique. The FELA provides both upper bound (UB) and lower bound (LB) estimations which can be used to represent the actual collapse load. The difference between bounds provides the exact amount of error in the solution and is further used to refine the mesh until the accurate collapse load is evaluated based on the adaptive mesh refinement technique (Sloan 2013). Thereafter, the collapse load is the average of the LB and UB solutions which leads to the exact solution. In FELA, a rigid-perfectly plastic material is effectively utilised to investigate the ultimate pressure applied at the top of open caissons. In the LB method, three-node triangular elements are used in the analysis. Each triangular element has the four nodal stresses which are set to be the basic unknown variables. The statically admissible stress discontinuities are allowed for producing the continuity of normal and shear stresses along with the interfaces of all the elements. The conditions of stress equilibrium, stress boundary condition and the Tresca failure criterion are all constraints in a typical LB analysis, in which the objective function is to maximise the collapse load of problems. The upper bound theorem requires a kinematically admissible velocity field where the external work is greater or equal to the plastic shear dissipation. In the UB method, six-node triangular elements are used in the formulation. At each node of the element, there are the horizontal and vertical velocities defined as the basic unknown variables. The setting of kinematically admissible velocity discontinuities is applied at the interfaces of all the elements. The Tresca material is set to obey the associated flow rule which is satisfied along any velocity discontinuity. These LB and UB theorems are perfectly fitted to the nonlinear programming optimisation problems using the second-order cone programming (SOCP). The constraints involved in this procedure are nonlinear and non-smooth but remain convex and amenable to analysis. More details of the formulation can be found in Sloan (2013). In this paper, the latest development of the FELA technique, which is OptumG2 FELA software (OptumCE 2015), is carried out to numerically solve the ultimate bearing capacity of the open caisson (q_u) which is later normalised by the soil cohesion (c) to be the N_c^* factor (see Equation (2)). FELA adopts the adaptive mesh which is optimised to get the accurate solutions. In the study, the adaptive iterations are set as 5, the number of elements is set as 10,000 based on the sensitivity analysis of mesh size (Keawsawasvong 2022; Chouhan et al. 2023). The typical mesh configuration adopted in the FELA of open caisson is shown in Figure 2.

4. Results and discussion

4.1. Bearing capacity of rough cutting edge

The FELA results of Case A are demonstrated in Figure 3. Note that all results hereafter are the average solutions from LB and UB methods. In this case, the cutting edge is fully embedded representing the shallow sinking. It can be found that the undrained bearing capacity factor (N) varied smoothly with the r_i/r_o ratio for both β = 30° and 45°. The bearing capacity factor is higher for the steeper cutting edge (β = 30°) compared to cutting edge with β = 45° for all variations in the radii ratio. An increase in the r_i/r_o ratio results in a decrease in N. Similar observations were reported by Chavda and Dodagoudar (2022a) for the case of ring footings resting on clays and Chavda and Dodagoudar (2022b) for the case of embedded cutting edge of caisson in clays. To validate the FELA results, the present results are compared with the existing solutions of cutting edge of caisson in drained clays from Chavda and Dodagoudar (2022b). It should be mentioned that the results from Chavda and Dodagoudar (2022b) were obtained using the displacement-based finite element method and the friction angle of soil was ϕ = 5°. However, the present study is the cases with ϕ = 0° (undrained condition). Therefore, the present solutions are lower than those of Chavda and Dodagoudar (2022b) due to the lower value of friction angle.

4.2. Rough cutting edge and smooth steining

4.2.1. Fully embedded caisson

Figure 4 shows the results of Case B, where the dimensionless parameter d/B representing the full embedment of caisson is varied as

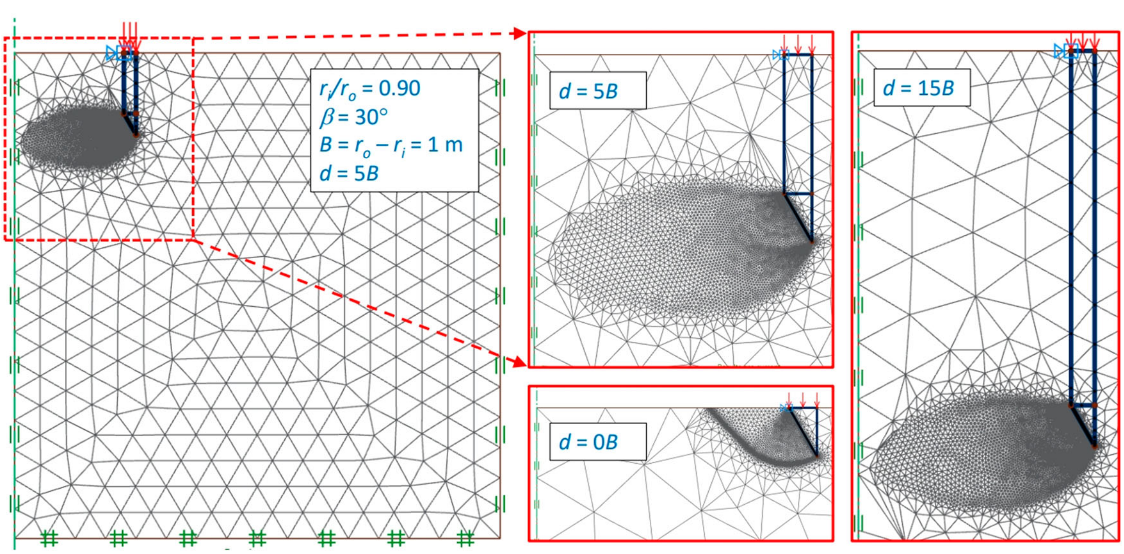

Figure 2. Typical mesh configuration adopted in the FELA axisymmetric model of circular open caisson with varying embedded conditions. (This figure is available in colour online.)

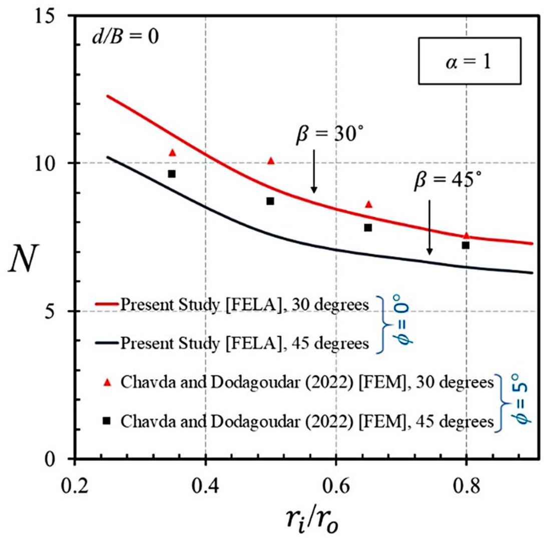

Figure 3. Comparison of bearing capacity factor N_c^* with literature. (This figure is available in colour online.)

0*B*, 1*B*, 5*B*, 10*B*, 15*B* and 20*B*. For both cutting angles ($\beta = 30°$ and 45°), when *d/B* reaches to 5, the effect of *d/B* becomes insignificant since the lines of *d/B* = 5, 10, 15 and 20 merges with each other. It is because when the depth of the caisson is deep and the wall interface is assumed to be smooth conditions, the slip lines of failure zones are mainly located at the tip of the cutting edge without an extension of the slip lines to the ground surface. Thus, influence of the caisson depth is no longer significant when the ratio of depth per thickness *d/B* is larger than 5. It should be also mentioned that the lines of *N* for the cases with $d/B \geq 1$ turn to be increased when the r_i/r_o ratio is larger than 0.6.

4.2.2. Embedded caisson with partial soil within caisson

Figure 5 shows the results of Case C, where the excavated ratio *d'/B* is considered as 0*B*, 5*B*, 10*B*, 15*B* and 20*B* and the value of *d/B* is fixed as 20. Generally, the effect of *d'/B* is insignificant when the r_i/r_o ratio is lesser than 0.6. The impact of *d'/B* is prominent when the thickness of open caissons is larger ($r_i/r_o > 0.7$). The effect of the removal of clay within caisson on the undrained bearing capacity factor of the cutting edge is almost insignificant. Therefore, the capacity of undrained clay to withstand the load of cutting edge and steining depends directly on the undrained cohesion. If the caisson is in equilibrium (caisson is not sinking) and the soil is removed within the caisson, the limiting capacity of soil being constant, the caisson will not sink further unless the undrained cohesion is completely mobilised. Moreover, if the undrained cohesion is mobilised, the caisson comes to an unstable state, and it will keep on sinking provided that the steining is smooth from within and outside. Therefore, the interface or side friction plays a significant role to allow control over the sinking of the caisson. To understand more about the observations for the Cases B and C, it can be related to the case where a piece of heavy rock is dropped on a very soft bed of fully saturated clay. The rock keeps on sinking in the clay (unstable case) when the weight of rock is higher than the overall undrained shear resistance offered by the soft undrained clay to the surface of rock.

4.3. Rough cutting edge and rough steining

4.3.1. Fully embedded caisson

The results of Case D for the open caisson with a purely rough interface are presented in Figure 6. Unlike Case B, the results of *N* are fluctuated and not merged into each other. This is due to the impact of the rough interface at the side of the wall. An increase in *d/B* yields an increase in the capacity of caissons, just like in the case of pile foundations. For the cases with small *d/B* values, the tendency of the *N* values is non-linearly decreased. On the other hand, when the ratio *d/B* increases to 15, the tendency of the *N* values becomes non-linearly increased. When the caissons are sunk to the required depth, there will be control over the sinking rate due to additional skin resistance provided by the undrained clay to the caisson through steining. Therefore, the sinking of caisson in undrained clay shall be done carefully and controlled by not using the lubrication between the steining and soil. This will allow to have a control over the sinking of caisson. This case is applicable to such clay which is homogeneous and isotropy is maintained in shear strength (i.e. the undrained shear strength of clay is not increasing with depth).

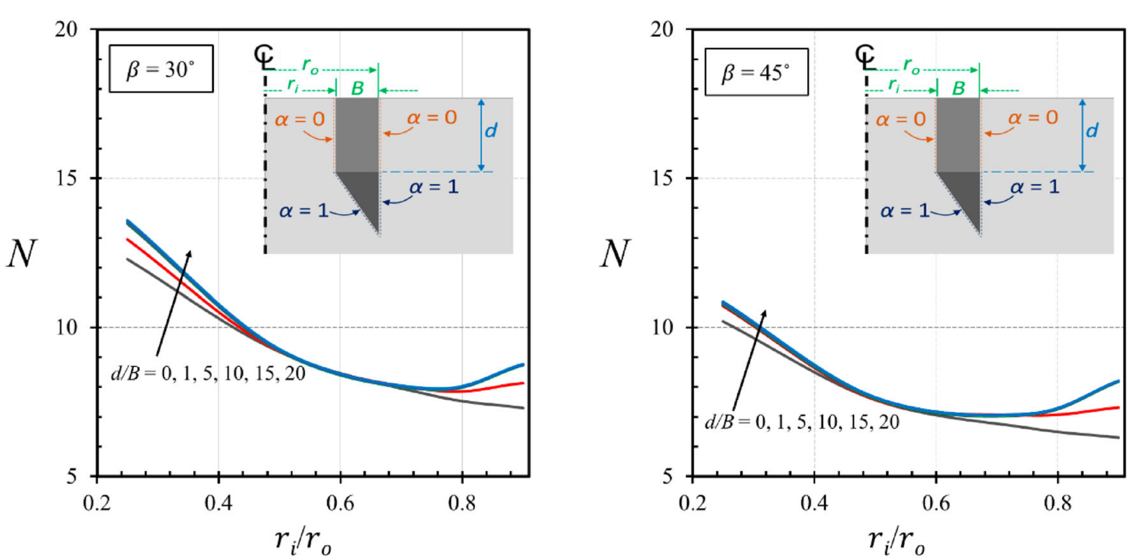

Figure 4. Undrained bearing capacity factor for fully embedded circular open caisson having smooth steining, varying radii ratio and rough cutting edge with varying cutting angles: (a) $\beta = 30°$ (b) $\beta = 45°$. (This figure is available in colour online.)

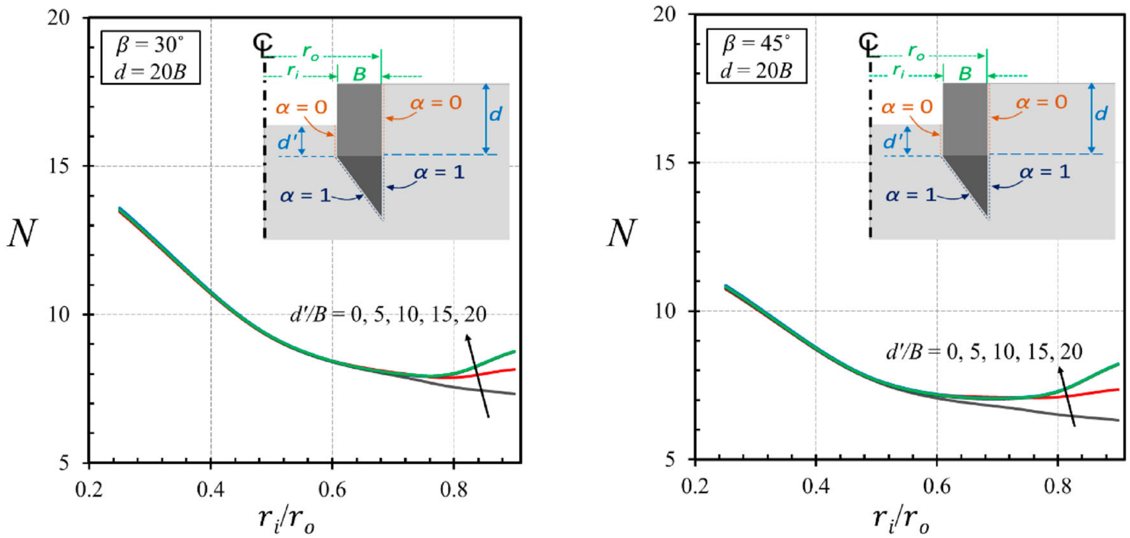

Figure 5. Undrained bearing capacity factor for embedded circular open caisson with partial soil within caisson having smooth steining, varying radii ratio and rough cutting edge with varying cutting angles: (a) $\beta = 30°$ (b) $\beta = 45°$. (This figure is available in colour online.)

4.3.2. Embedded caisson with partial soil within caisson

The results of Case E for the rough open caisson with partially excavated soil inside are presented in Figure 7. Note that the value of d/B is 20. Generally, the tendency of the N values is similar to that of Case D. There is a slightly difference from Case D when the r_i/r_o ratio is lesser than 0.5, where the lines of $d'/B = 5$, 10, 15 and 20 seem to be merged. When the caisson is already sunk to a depth of $d = 20B$ and if further sinking is required, the removal of internal soil will allow the further sinking as the N reduces with the removal of soil d'/B from 0B to 20B. These observations when compared with the Case C, where the steining is completely smooth and soil is removed within caisson, there will not be the control over the sinking of caisson. Therefore, it is stated that the roughness of steining plays a significant role in having the control over the sinking of caisson in clay.

4.4. Failure planes for open caisson

Figures 8–10 show the typical failure planes for the open caisson representing the failure mechanism corresponding to the effect of radii ratio and embedment depth, removal of soil within the caisson and cutting angles of the open caisson, respectively. Figure 8 shows the failure planes representing the effect of radii ratio and embedment depth for $\beta = 30°$ and $d'/B = 20$. It is observed from the figure that an increase in the r_i/r_o ratio the failure planes transform from overall failure to local failure due to a reduction in the confinement thereby resulting in the decrease in N. Similar observations were reported by Chavda and Dodagoudar (2022a) for the case of ring footings resting on clays. Additionally, there is a significant effect of d/B varying from 0 to 15B, due to increase in the size of failure planes. Figure 9 shows the failure planes representing the effect of excavated ratio d'/B varied from 0 to 20B for $r_i/r_o =$ 0.90, $\beta = 30°$ and $d/B = 20$. It is observed from the figure that as

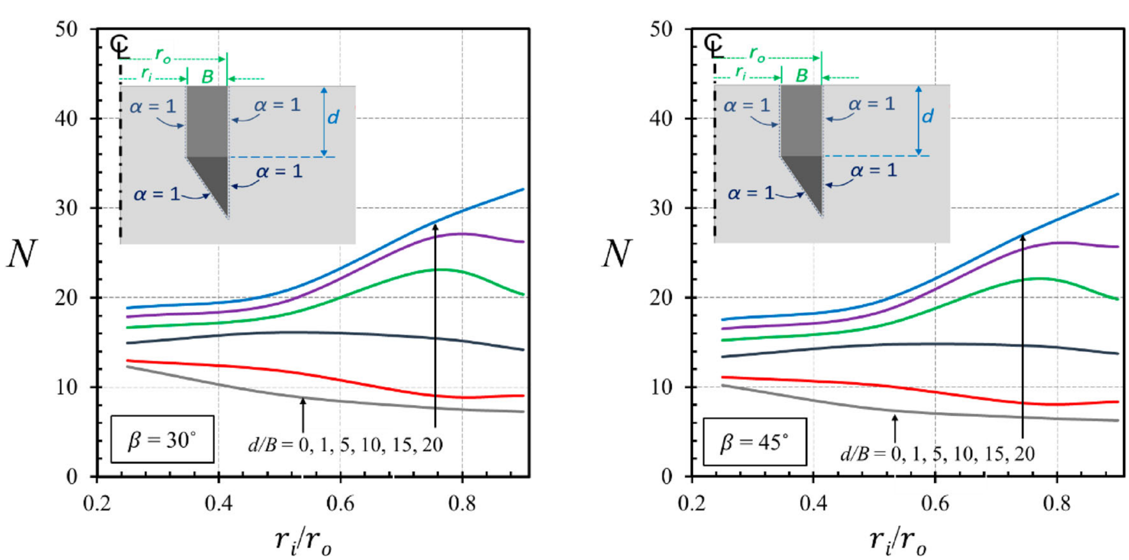

Figure 6. Undrained bearing capacity factor for fully embedded circular open caisson having rough steining, varying radii ratio and rough cutting edge with varying cutting angles: (a) $\beta = 30°$ (b) $\beta = 45°$. (This figure is available in colour online.)

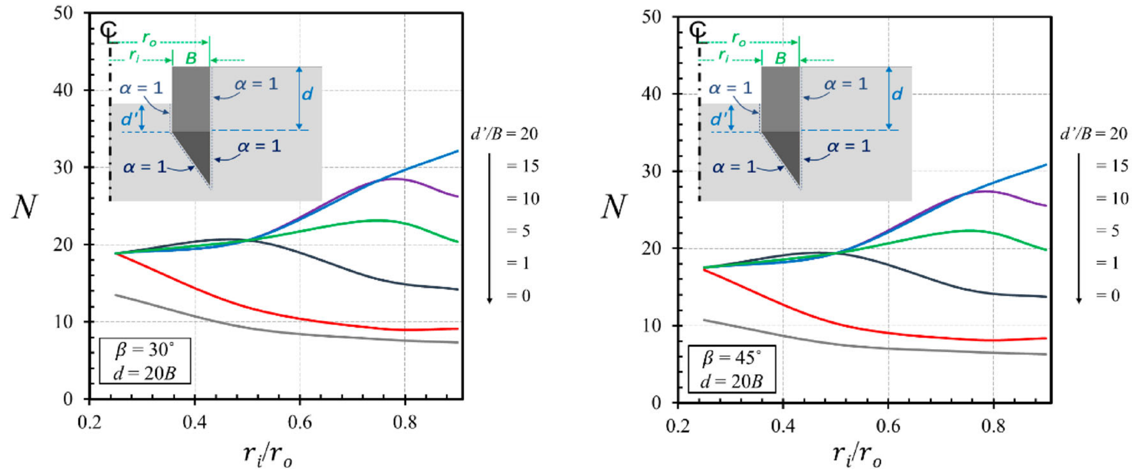

Figure 7. Undrained bearing capacity factor for embedded circular open caisson with partial soil within caisson having rough steining, varying radii ratio and rough cutting edge with varying cutting angles: (a) $\beta = 30°$ (b) $\beta = 45°$.

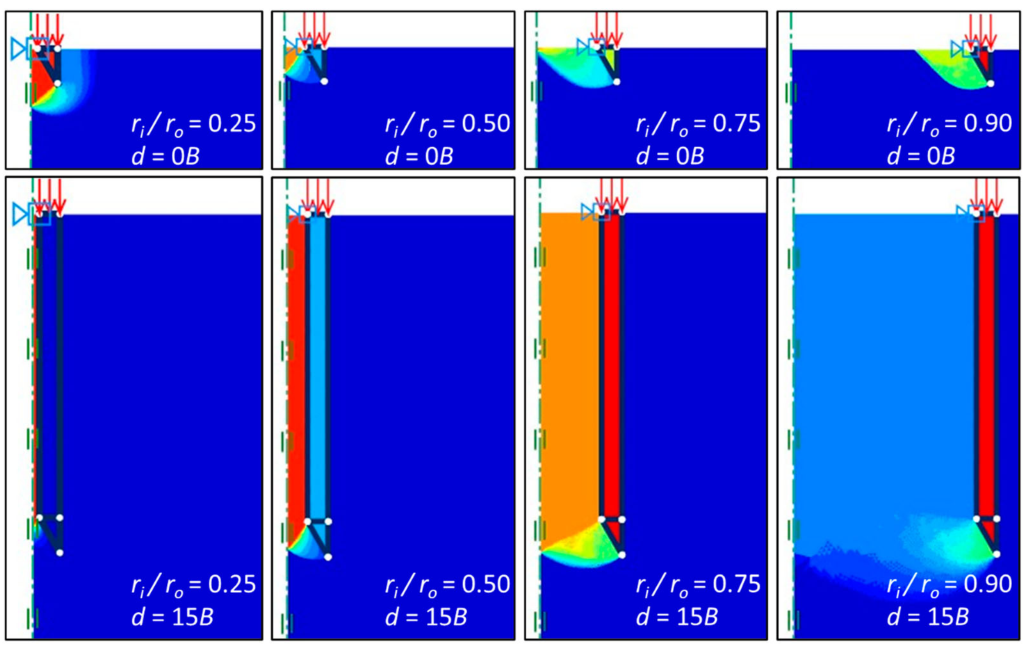

Figure 8. Effect of radii ratio and embedment depth of caisson for Case A and B with $\beta = 30°$ and $d'/B = 20$ on the development of failure plane. (This figure is available in colour online.)

the clay is removed within the caisson from $20B$ to 0, the failure zones extent to the ground surface and therefore, significantly affect the bearing capacity factor. However, the effect of d'/B becomes insignificant when $d'/B \geq 5$ as the failure planes are not much influenced and are developed fully near the cutting edge only. Figure 10 shows the failure planes representing the effect of the cutting angle of $\beta = 30°$ and 45° for $r_i/r_o = 0.25$ and 0.90, $d/B = 0$ and $20B$, and $d'/B = 20B$. It is observed from the figure that the effect of β on failure planes for steeper cutting edge ($\beta = 30°$) is wider and deeper as compared with $\beta = 45°$ and therefore, the bearing capacity factor is higher for the steeper cutting edge ($\beta = 30°$) compared to cutting edge with $\beta = 45°$. Similar observations were reported by Chavda and Dodagoudar (2022b).

5. Conclusions

In the study, the undrained bearing capacity factor N of the cutting edge is evaluated using finite element limit analysis (FELA) considering different cutting angles of cutting edge, varying embedment and radii ratio of caisson, different depths of removal of soil within caisson, and different roughness conditions of steining. For the case of shallow embedment of caisson, FELA study results are compared with those available in the literature. The present study results will be useful in evaluating the stability of circular open caisson when sunken in clayey soils. The conclusions drawn from the FELA-based study are as follows.

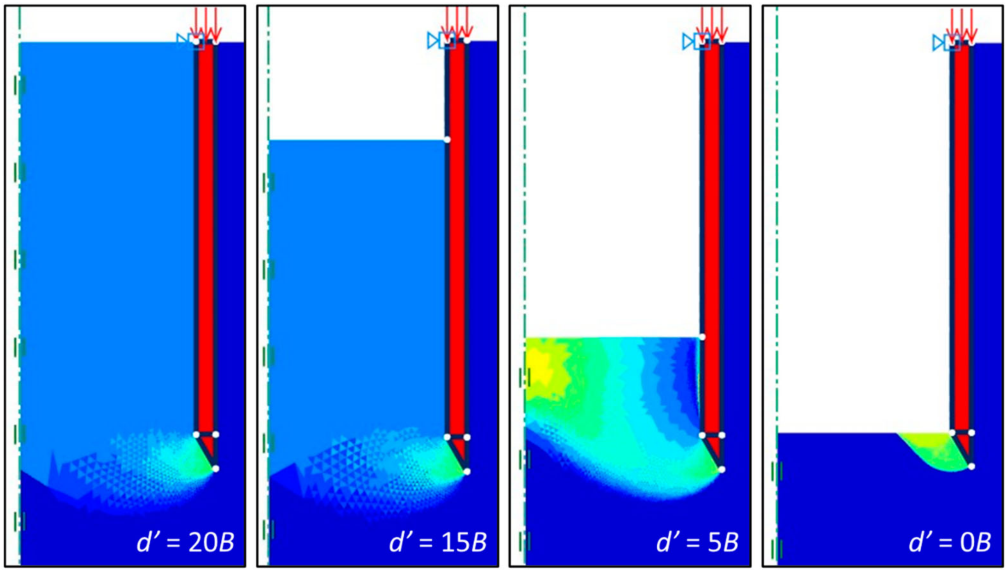

Figure 9. Effect of removal of soil within caisson for Case C with $r_i/r_o = 0.90$, $\beta = 30°$ and $d/B = 20$ on the development of failure plane. (This figure is available in colour online.)

- For the shallow embedment of caisson, the undrained bearing capacity factor N is higher for the cutting edge with $\beta = 30°$ compared to $\beta = 45°$ for all radii ratio variations ($r_i/r_o = 0.25$ to 0.9). For the other cases too, where the embedment of the caisson is varied, the depth of soil within caisson is varied representing the removal of soil, the undrained bearing capacity factor is higher for cutting edge with $\beta = 30°$ compared to $\beta = 45°$.
- For the case when only the cutting edge is fully embedded, the undrained bearing capacity factor N of the cutting edge reduces with an increase in the radii ratio of the cutting edge. For caisson with different embedment ($d/B = 1$ to 20), the undrained bearing capacity factor reduces with an increase in the r_i/r_o up to 0.65. The slight dependency of the embedment ratio of caisson on the undrained bearing capacity factor is observed for $r_i/r_o > 0.65$. This may be attributed due to the change in the failure mechanism which is shifted from an overall failure mechanism to a local failure mechanism for $r_i/r_o > 0.65$.
- The caissons during sinking can have smooth and rough steining conditions. The undrained bearing capacity of the cutting edge is highly influenced by the roughness of steining. When the steining is completely smooth, the undrained bearing capacity factor is almost same for the variation in different embedment of caisson and variation in the depth of removal of soil within caisson. Therefore, when sinking caissons in clay, if the lubrication is used to make the steining smooth, it will be difficult to have control over the sinking of a caisson. Whereas, when the sides of

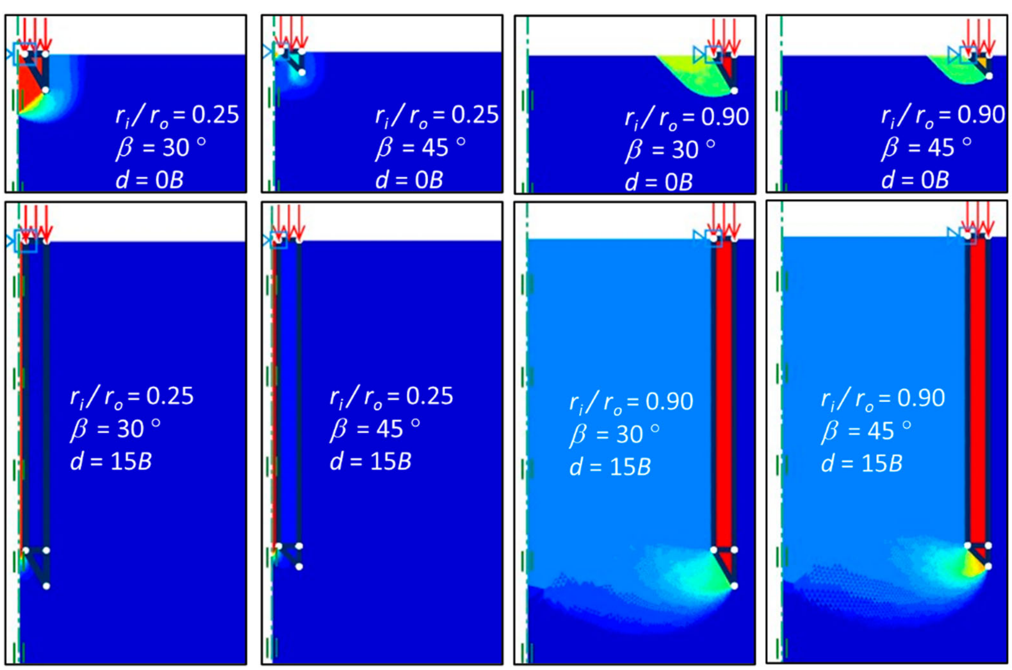

Figure 10. Effect of cutting angles of cutting edge for Case A and B with $r_i/r_o = 0.25$ and 0.90 and $d'/B = 20$ on the development of failure plane. (This figure is available in colour online.)

steining are rough, the undrained bearing capacity factors are influenced resulting to have control over the sinking of caissons.

- With the removal of soil within embedded caissons, the undrained bearing capacity factor reduces and reaches to the case where only the cutting edge is embedded for both cases of steining being smooth and rough. The presence of soil outside the caissons does not influence the undrained capacity of cutting edge when steining is smooth. However, the undrained capacity of caisson is influenced by the roughness of the steining.
- The typical failure planes for the open caisson are evaluated representing the failure mechanism accounting the effect of radii ratio and embedment depth, removal of soil within the caisson and cutting angles of the open caisson. It is inferred that the failure planes transform from overall failure to local failure with increase in the r_i/r_o ratio thereby resulting in the decrease in the N. There is a significant effect of embedment depth (d/B) due to increase in the size of failure planes. The removal of clay within the caisson (d'/B) affects the bearing capacity factor, however, the effect of d'/B becomes insignificant when $d'/B \geq 5$ as the failure planes are not much influenced and are developed fully near the cutting edge only. The developed failure planes are wider and deeper for steeper cutting edge ($\beta = 30°$) as compared to flatter cutting edge ($\beta = 45°$) and therefore, the N is higher for the steeper cutting edge.

Acknowledgements

This study was financially supported by Office of the Permanent Secretary, Ministry of Higher Education, Science, Research and Innovation under Research Grant for New Scholar (RGNS 65-112).

Disclosure statement

No potential conflict of interest was reported by the author(s).

Funding

This study was financially supported by Office of the Permanent Secretary, Ministry of Higher Education, Science, Research and Innovation under Research Grant for New Scholar (RGNS 65-112).

Data availability statement

All data, models, or code that support the findings of this study are available from the corresponding author upon reasonable request.

ORCID

Jitesh T. Chavda http://orcid.org/0000-0003-0396-5759
Suraparb Keawsawasvong http://orcid.org/0000-0002-1760-9838
Phadungsak Rattanadecho http://orcid.org/0000-0002-9766-617X

References

Allenby D, Waley G, Kilburn D. 2009. Examples of open caisson sinking in Scotland. Proc Inst Civil Eng Geotech Eng. 162(1):59–70. doi:10.1680/geng.2009.162.1.59.

Berezantsev. 1952. Axisymmetric problem of the theory of limiting equilibrium of granular media. Gosstroiizdat, Moscow [in Russian].

Caquot A, Kérisel J. 1953. Sur le terme de surface dans le calcul des fondations en milieu pulvérulent. 3rd International Conference on Soil Mechanics and Foundation Engineering, Zurich, vol. 1, 336–337. CRID 1573105974661112320.

Chakrabarti SK, Chakrabarti P, Krishna MS. 2006. Design, construction, and installation of a floating caisson used as a bridge pier. J Waterw Port Coast Ocean Eng. 132(3):143–156. doi:10.1061/(ASCE)0733-950X(2006)132:3(143).

Chavda JT, Dodagoudar GR. 2018. Finite element modelling of extent of failure zone in c-ϕ soil at the cutting edge of open caisson. In: Cardoso A, Borges J, Costa P, Gomes A, Marques J, Vieira C, editors. Numerical methods in geotechnical engineering IX. Porto, Portugal: CRC Press; p. 999–1007. ISBN9780429446924.

Chavda JT, Dodagoudar GR. 2021. Experimental evaluation of failure zone in sand beneath the ring footing and cutting edge of open caisson using image analysis. In: Patel S, Solanki CH, Reddy KR, Shukla SK, editors. Proceedings of the Indian geotechnical conference 2019. Singapore: Springer; p. 273–283. doi:10.1007/978-981-33-6346-5_24.

Chavda JT, Dodagoudar GR. 2022a. Experimental studies on a circular open caisson. Int J Phys Model Geotech. 22(2):70–87. doi:10.1680/jphmg.20.00050.

Chavda JT, Dodagoudar GR. 2022b. Finite element evaluation of bearing capacity factors for cutting face of open caissons. Int J Geotech Eng. 16(8):951–961. doi:10.1080/19386362.2022.2080962.

Chavda JT, Mishra S, Dodagoudar GR. 2020. Experimental evaluation of ultimate bearing capacity of the cutting edge of an open caisson. Int J Phys Model Geotech. 20(5):281–294. doi:10.1680/jphmg.18.00052.

Chouhan K, Lai VQ, Chavda JT, Yoonirundorn K, Keawsawasvong S. 2023. Evaluation of vertical bearing capacity factors for conical footing with varying base roughness using FELA and MARS model. Ships Offsh Struct. 0:1–13. doi:10.1080/17445302.2023.2177030.

Dammala PK, Bhattacharya S, Krishna AM, Kumar SS, Dasgupta K. 2017. Scenario based seismic re-qualification of caisson supported major bridges - A case study of saraighat bridge. Soil Dyn Earthq Eng. 100:270–275. doi:10.1016/j.soildyn.2017.06.005.

de Beer EE. 1970. Experimental determination of the shape factors and the bearing capacity factors of sand. Géotechnique. 20(4):387–411. doi:10.1680/geot.1970.20.4.387.

Dong X, Guo M, Wang S. 2023. Inclination prediction of a giant open caisson during the sinking process using various machine learning algorithms. Ocean Eng. 269:113587. doi:10.1016/j.oceaneng.2022.113587.

Esteban Lefler F, Rey Romero VD. 2009. Reinforced concrete caissons for port structures in Spain. Proc Inst Civil Eng Maritime Eng. 162(2):73–81. doi:10.1680/maen.2009.162.2.73.

Griffiths DV. 1982. Computation of bearing capacity factors using finite elements. Géotechnique. 32(3):195–202. doi:10.1680/geot.1982.32.3.195.

Hansen JB. 1961. A general formula for bearing capacity. Copenhagen: B 11, B Geoteknisk Institut, The Danish Geotechnical Institute.

IRC: 78. 2000. Standard specifications and code of practice for road bridges. New Delhi: The Indian Roads Congress.

IS: 3955. 1965. Code of practice for design and construction of well foundations. New Delhi: Bureau of Indian Standards.

IS: 9527, Part 1. 1981. Code of practice for design and construction of port and harbour structures, part 1 concrete monoliths. New Delhi: Bureau of Indian Standards.

Jiang BN, Yu T, Peng WM, Zhang YB, He SB, Ma JL. 2023. Analysis of mechanism of sand gushing and sudden sinking of ultra-large deep-water open caisson in sand via field and model tests. Appl Ocean Res. 130:103436. doi:10.1016/j.apor.2022.103436.

Keawsawasvong S. 2022. Bearing capacity of conical footings on clays considering combined effects of anisotropy and non-homogeneity. Ships Offsh Struct. 17(1):2317–2328. doi:10.1080/17445302.2021.1987110.

Matsuda T, Maeda K, Miyake M, Miyamoto J, Sumida H, Tsurugasaki K. 2016. Instability of a caisson-type breakwater induced by an earthquake–tsunami event. Int J Geomech. 16(5):C4016003. doi:10.1061/(ASCE)GM.1943-5622.0000619.

Meyerhof GG. 1963. Some recent research on the bearing capacity of foundations. Can Geotech J. 1(1):16–26. doi:10.1139/t63-003.

Nayak NV. 1985. Foundation design manual. New Delhi: Dhanpat Rai and Sons Pub.

Nonveiller E. 1987. Open caissons for deep foundations. J Geotech Eng. 113(5):424–439. doi:10.1061/(ASCE)0733-9410(1987)113:5(424).

OptumCE. 2015. OptumG2. Optum Computational Engineering. Copenhagen, Denmark.

Royston R, Phillips BM, Sheil BB, Byrne B. 2016. Bearing capacity beneath tapered blades of open dug caissons in sand. Civil Engineering Research, Ireland 2016.

Royston R, Sheil B, & W B, Byrne B. 2022b. Monitoring the construction of a large-diameter caisson in sand. Proc Inst Civil Eng Geotech Eng. 175(3):323–339. doi:10.1680/jgeen.19.00266.

Royston R, Sheil BB, Byrne BW. 2022a. Undrained bearing capacity of the cutting face for an open caisson. Géotechnique. 72(7):632–641. doi:10.1680/jgeot.20.P.210.

Sheil B, Royston R, Byrne B. 2018. Real-time monitoring of large-diameter caissons. Proceedings of China-Europe Conference on Geotechnical Engineering: Volume 1, 725–729. Springer International Publishing. doi:10.1007/978-3-319-97112-4_162.

Sheil B, Templeman J. 2022. Bearing capacity of open caissons embedded in sand. Géotechnique. 73(6):495–505. doi:10.1680/jgeot.21.00089.

Sloan SW. 2013. Geotechnical stability analysis. Géotechnique. 63:531–572. doi:10.1680/geot.12.RL.001.

Solov'ev NB. 2008. Use of limiting-equilibrium theory to determine the bearing capacity of soil beneath the edges of caissons. Soil Mech Found Eng. 45 (2):39–45. doi:10.1007/s11204-008-9006-z.

Templeman JO, Phillips BM, Sheil BB. 2021. Cutting shoe design for open caissons in sand: influence on vertical bearing capacity. Proc Inst Civil Eng Geotech Eng. 176(1):58–73. doi:10.1680/jgeen.20.00218.

Terzaghi K. 1943. Theoretical soil mechanics. New York: John Wiley and Sons.

Tomlinson MJ. 2001. Foundation design and construction, 7th ed. Harlow: Prentice Hall.

Vesic AA. 1973. Analysis of ultimate loads of shallow foundations. J Soil Mech Found Div ASCE. 99(1):45–73. doi:10.1061/JSFEAQ.0001846.

Yan FY, Guo YC, Liu SQ. 2011. The bearing capacity analyses of soil beneath the edge of circular caisson. Adv Mat Res. 250:1794–1797. doi:10.4028/www.scientific.net/AMR.250-253.1794.

Yao Q, Yang XG, Li HT. 2014. Construction technology of open caisson for oversize surge shaft in drift gravel stratum. Electron J Geotech Eng. 19:5725–5738.